Environ. Sci. Technol. **1997**, *31*, 1313−1319

Expression Dewatering of Alum-Coagulated Clay Slurries

I. L. CHANG,† C. P. CHU,† D. J. LEE,*,† AND CHIHPIN HUANG‡

Department of Chemical Engineering, National Taiwan University, Taipei, Taiwan, 10617, Republic of China, and Institute of Environmental Engineering, National Chiao Tung University, Hsinchu, Taiwan, 30039, Republic of China

Filtration followed by expression characteristics of the alum-coagulated clay slurries are first reported in this paper. A strong correlation between alum chemistry and the dewatering efficiency exists. At pH 3, where the positively charged ions are the dominating species, the alum addition has only a minor improvement on dewatering efficiency. At pH 7 and pH 10, where sweep flocs enmeshment play the major role, dewatering performance improves continuously as alum dose increases. At pH 5.2, where a charge reversal regime exists, the dewatering efficiency exhibits a reversal phenomenon as well. The overall dewaterability follows: pH 5.2 > pH 3 > pH 7 > pH 10. A complete test consists of the filtration and expression stages, which are discussed separately. The filtration stage is discussed based on the average specific resistance and the residual moisture in the filtration cake. The expression stage is discussed based on the combined Terzaghi−Voigt rheological model, from which the fraction contributed by the secondary consolidation (B) and the particle creeping factor (η) are evaluated. For the dewatering sake, a lower B and a higher η are desired. Both parameters B and η increase at elevated alum dose and/or lower pH value, while exhibiting a local minimum in charge reversal regime at pH 5.2. The optimal alum dose considering sludge dewaterability is discussed.

Introduction

Alum coagulation has long been widely employed for water treatment. Precipitation-charge neutralization (PCN) and sweep flocs enmeshment are proposed as the two major mechanisms in coagulating the constituting particles into larger flocs (*1*−*7*). The former is dominating at pH 5−6; while the latter dominates in nearly neutral to high pH regime (*8*, *9*). The so-called "optimal alum dose" is usually located at such a specific dose where the slurry supernatant residual turbidity or some target species concentration (such as humic acids) reaches a minimum (*10*).

Due to the relatively low energy consumption rate when compared with the thermal dewatering methods, expression has been employed in industries to separate the liquid from a cake by a mechanical pressure (*11*). One of the major applications is in water and wastewater sludge treatments, such as the belt filter press or screw press (*12*, *13*). In the past 3 decades, much research work on constant-pressure expression were accomplished by Shirato and Murase (*14*−*19*) and Tiller (*11*, *20*). Yeh (*21*) and Tong (*22*) have provided a brief literature review. Investigation about constant-pressure expression can provide a basic understanding of detailed mechanisms involved and implications to the design and operation of sludge dewatering.

Although alum has been widely employed in water treatment practice, filtration followed by expression dewatering of alum-coagulated slurries has not been investigated. In this paper, we discuss separately the effects of alum dosage on the filtration stage and the expression stage characteristics of clay slurry. Often the slurry coagulation step is considered independently of the dewatering step. We investigated herein the so-called "optimal alum dose criterion" considering sludge dewaterability as well.

Experimental Section

Clay powder (U.K. ball clay) was the testing material. The particle size distribution was determined by Sedigraph 5100C (Micromeritics) as a monodispersed distribution with a mean diameter of approximately 4.6 μm. The true solid density was measured by Accupyc Pycometer 1330 (Micrometritics), giving a measure of 2584 kg/m^3 with a relative deviation of less than 0.5%. The suspension was prepared by mixing clay particles with distilled water, with the addition of 10^{-1} M $NaClO_4$. (Note: The ClO_4^- ions have been recognized as an indifferent ion in the adsorption field, which is therefore used in order to reduce the anion effect on the interaction between alum and clay surface.) The solution pH values were then adjusted by $HClO_4$ and NaOH. The mixing unit was a baffled mixing chamber with a stirrer. After the weighed powder was suspended in the solution, the alum solution was then gradually poured into the mixing vessel with 200 rpm of stirring for 5 min followed by 50 rpm for another 20 min. Alum dosages ($Al_2(SO_4)_3 \cdot 14H_2O$) ranged from 0 to 1000 ppm. Clay weight percentage in the suspension was 20%. Such a concentration level is much higher than what appears in usual surface water. Discrepancies would exist between the present slurry and that from surface water treatment. However, we expect that the major conclusions drawn from the former would be applicable to the latter.

A set of jar tests was conducted to measure the residual turbidity of the conditioned slurry after 120 min of settling. The number of pH/dose combinations is 80 (pH 3, 4, 5, 6, 7, 8, 9, and 10 and alum dose of 0, 100, 200, 300, 400, 500, 600, 700, 850, and 1000 ppm). Figure 1 represents the results, whose basic characteristics are the same as those suggested in ref 1. The turbidity generally decreases with increasing alum dose and decreasing pH. However, a reversal regime (a band between the two isopleths of 10 NTU) appears, especially around pH 6−7 (the regime R). According to the solubility calculation, the precipitate would not appear at pH 3, but should largely occur at pH 5−7 and when the alum dose is higher than approximately 900 ppm at pH 10.

After mixing and prior to settling, a small quantity of clay−alum aggregates in the vessel was transferred carefully into the fresh electrolyte at the same pH and electrolyte concentration as the original electrolyte. ζ potentials of clay−alum aggregates were then measured by the ζ meter (Zetasizer IIc, Malvern), which increases with increasing alum dosage at all pH values. The ζ potential isopleths are also depicted in Figure 1. The ζ potential changes from negative to positive at different alum dose under various pH values, for example, approximately 800 ppm at pH 3; 300 ppm at pH 5.2; 290 ppm at pH 7.0; and 820 ppm at pH 10.0. The zero ζ potential curve and the reversal region identified by turbidity measurement around pH 5−7 is noted (regime near point A), where PCN should play a major role (zone 2 coagulation). At elevated

* Corresponding author fax: 886-2-362-3040; e-mail: djlee@ccms.ntu.edu.tw.
† National Taiwan University.
‡ National Chiao Tung University.

S0013-936X(96)00532-9 CCC: $14.00

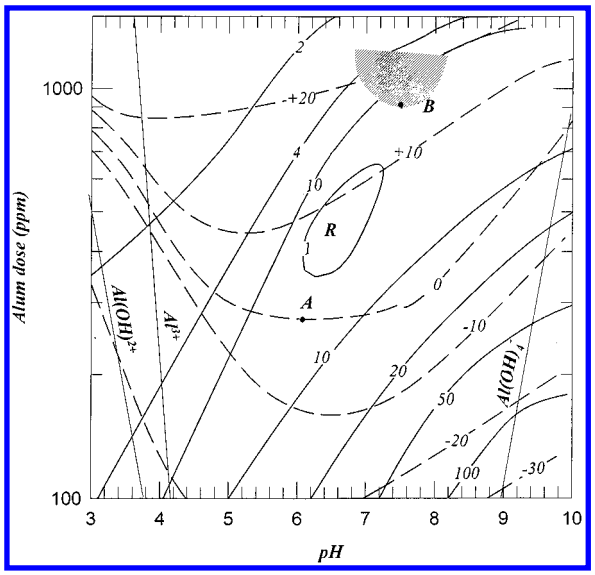

FIGURE 1. Alum solubility diagram with residual turbidity and ζ potential isopleths. Clay slurry, 20% w/w, 10^{-1} N. Shaded area, optimal sweep regime; R, charge reversal regime.

pH values where turbidity data show no correlation with the ζ potentials, the sweep flocs enmeshment mechanism may dominate (zone 4 coagulation). At pH 3, the amount of absorbed ions increases with alum dose, as evidenced by the increase in ζ potential.

The zone settling velocity (ZSV) was obtained from linear regression of sediment height versus time curve in these jar tests as well. The ZSV follows the sequence pH 5.2 > pH 7 > pH 3 > pH 10. The so-called "optimal sweep zone", where the flocs exhibit the best settling with the lowest coagulant dosages (*1*), is depicted as the shaded area in Figure 1. Point B corresponds to the lowest alum dosage to induce sweeping.

A constant head piston press (Triton Electronics Ltd., type 147) was employed for all expression tests. Figure 2 is a schematic drawing of the experimental setup. The sludge was placed in the inner stainless steel cylinder of diameter 7.62 cm and height 20 cm. Two pieces of Whatman No. 1 filter paper are the filter medium. A hydraulic pressure of 1000 psi was exerted onto the piston to force out the moisture. The electric balance connected to a personal computer automatically recorded the time evolution of filtrate weight. With the filtrate weight versus time data and the true solid density data, the time evolution of cake porosity can be subsequently obtained. The number of pH/dose combinations is 35 (pH 3, 5.2, 6, 7, and 10 and alum 0, 100, 300, 500, 700, 850, and 1000 ppm). For each expression test and jar test, more than three independent experiments were conducted to check the data reproducibility.

Results and Discussion

General. The results of expression for the coagulated clay by various dosages of alum at four pH conditions are expressed in Figure 3a–d, respectively. At pH 3, 7, and 10, as alum dose amount increases, the dewatering curve shifts to the left, reflecting an improvement of dewaterability. At pH 5.2, reversal occurs during the 400–700 ppm of alum dosage. Roughly speaking, the overall sludge dewaterability follows the sequence: pH 5.2 > pH 3 > pH 7 > pH 10. This is consistent with the conclusion drawn by Knocke et al. (*23*).

At pH 3, the original slurry has exhibited a better dewaterability owing to the lower charge carried on clay surface and subsequently the lower repulsion forces between clay particles than at other pH values. The presence of cationic species can thereby only slightly reduce the interparticle repulsion further, a minor, subsequent dewaterability improvement. At pH 7 and pH 10, where sweep flocs enmeshment becomes important as alum dose has exceeded solubility limit (less than 1 ppm for pH 7; 850 ppm for pH 10), the dewaterability improves progressively as alum dose increases. At pH 5.2, the dewaterability curve exhibits a reversal phenomenon, which corresponds to the charge reversal region identified by residual turbidity and 30 ζ potential in Figure 1.

A complete test includes the following two stages: the filtration and the expression stages, which are discussed individually. In this study, we adopt the method proposed by Shirato et al. (*14*) to locate the transition point separating these two stages. Figure 4 represents some examples. With the data in the left side of the separating point (indicated as region F in Figures 3 and 4), which corresponds to the filtration stage, we can evaluate the average specific resistance to filtration under 1000 psi pressure difference according to the procedures proposed by Leu (*24*). With the data in the right side of the separation point (region C in Figures 3 and 4), which corresponds to the expression stage, we can identify

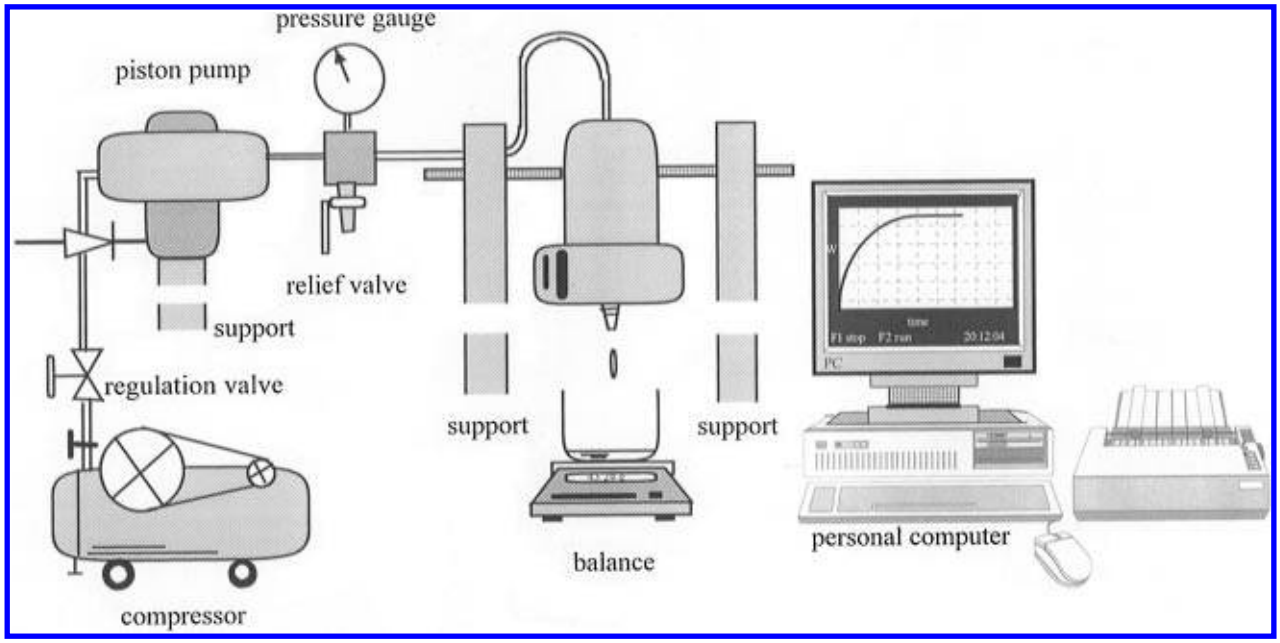

FIGURE 2. Experimental setup.

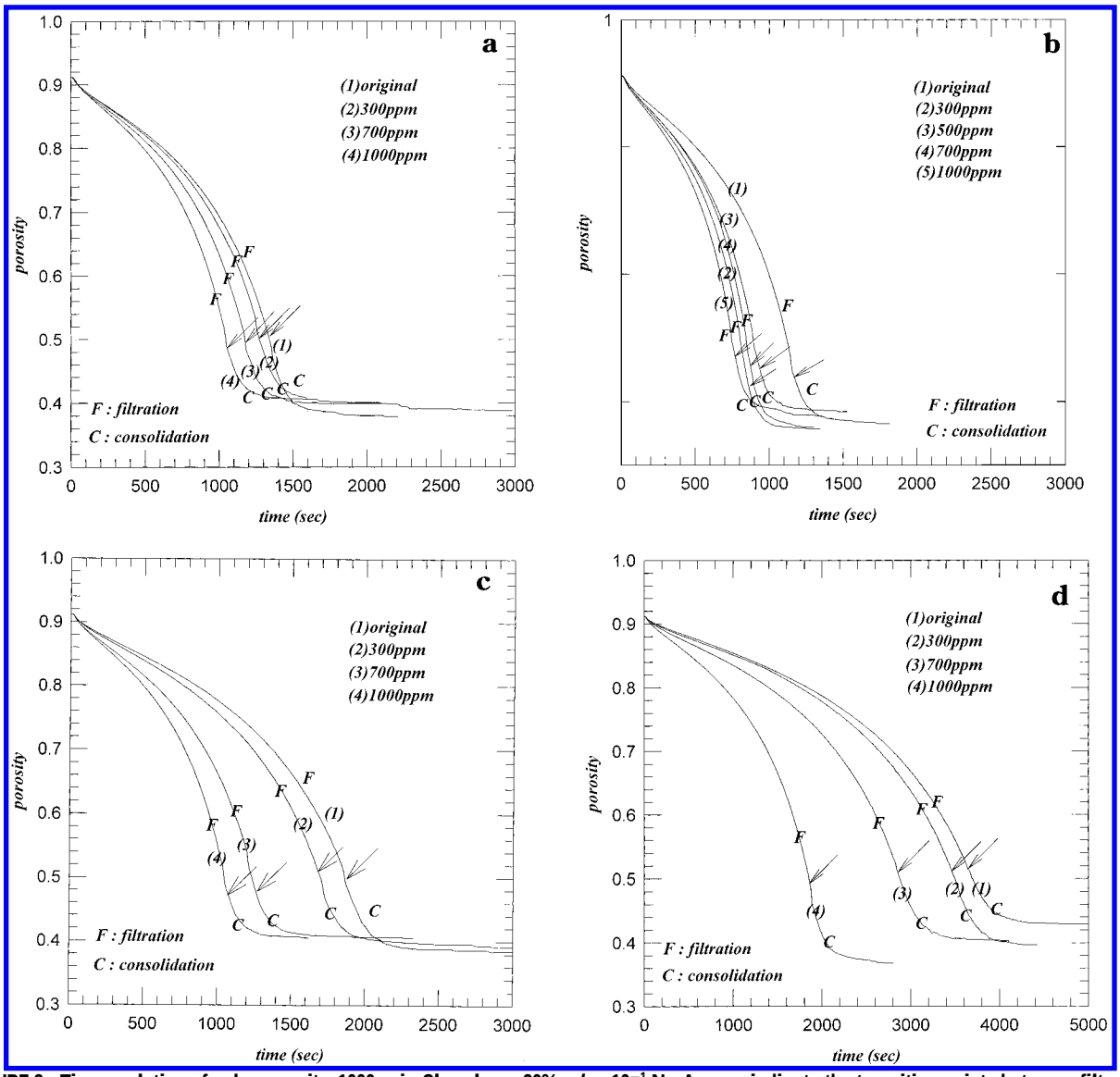

FIGURE 3. Time evolution of cake porosity, 1000 psi. Clay slurry, 20% w/w, 10^{-1} N. Arrows indicate the transition points between filtration and consolidation. (a) pH 3, (b) pH 5.2, (c) pH 7, and (d) pH 10.

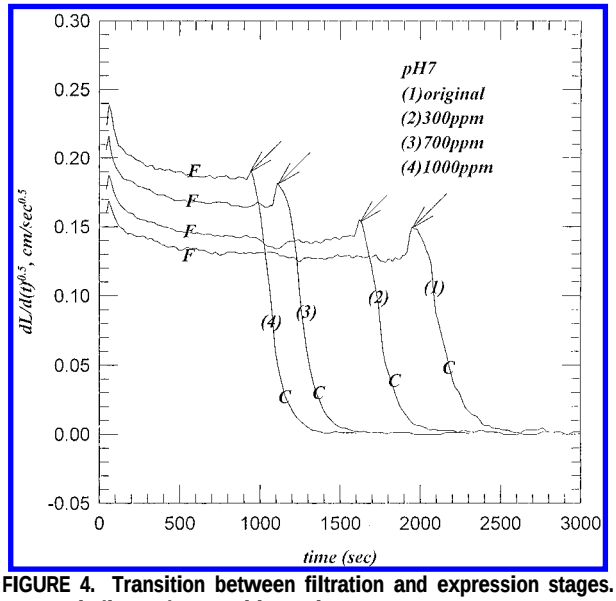

FIGURE 4. Transition between filtration and expression stages. Arrows indicate the transition points.

individually the primary and secondary consolidation stages (discussed later).

The packing status of constituting clay particles changes continuously during a test. In the slurry prior to settling, the clay particles may form large, loose, fractal-like aggregates due to the results of coagulation. To prevent confusions, such aggregates are termed as "flocs" here. During filtration and the subsequent expression stage, as the shear stress experienced by the constituting particles in consolidated cake is much higher than in suspension, the weaker structure in flocs would break down into smaller aggregates with much stronger *intra-aggregate* strength. These aggregates are termed as "aggregates" in further discussions to characterize the consolidated cake properties.

Filtration Stage. Figure 5 represents the average specific resistance data under 1000 psi constant-pressure filtration as alum dose increases. Apparently, the average specific resistance decreases with alum dose, thus reflecting a looser cake structure obtained. A reversal result is also noted around pH 5.2. As the constituting aggregate surfaces are near-neutral, the resulting cake structure will become looser (*25*), thereby permitting a higher filtration rate, which corresponds to the pH 3 and pH 5.2 results. At pH 7 and pH 10, the decrease in filtration resistance should be attributed to the constituting aggregate characteristics formed by sweep floc enmeshment mechanism. A low specific resistance is advantageous from the viewpoint of dewatering.

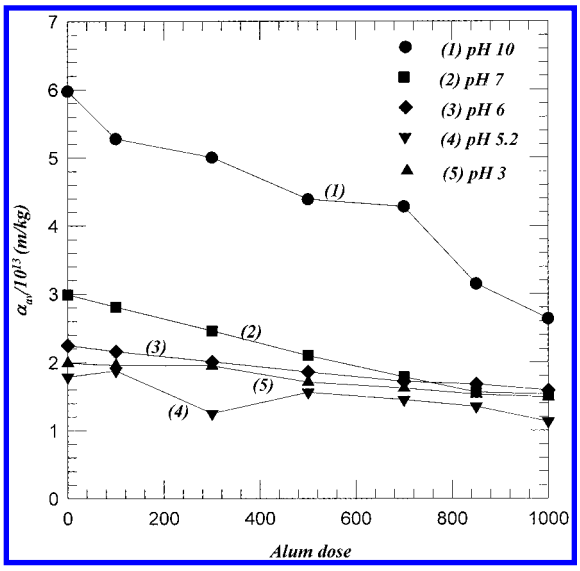

FIGURE 5. α_{av} versus alum dose. Clay slurry, 20% w/w, 10^{-1} N.

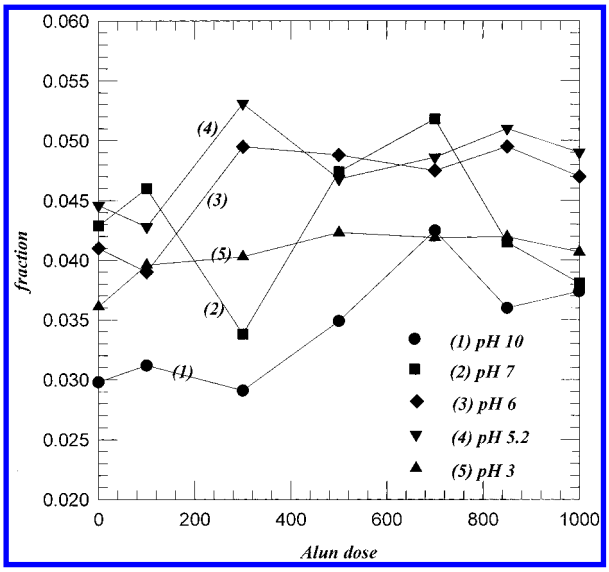

FIGURE 6. Fraction of moisture not removable in filtration stage versus alum dose. Clay slurry, 20% w/w, 10^{-1} N.

The separation points shown in Figure 4 are used to calculate the percentage of residual moisture after the filtrate stage (moisture remained in the cake at the end of filtration divided by the total moisture content). Figure 6 represents the fraction of residual moisture to the initial moisture versus alum dose. A higher fraction is noted at the corresponding lower average specific resistance region. This arises naturally because a loose neutralized cake would trap more moisture during filtration. A drop in fraction occurs in the 1000 ppm dose at pH 7 and pH 10, whose cause is not unclear. However, it should be attributed to the sweep floc mechanism under high alum dosage. From the viewpoint of sludge disposal, the higher residual moisture in cake after filtration is not favorable.

Expression Stage. The consolidation stage is differentiated from the filtration stage and is redrawn in Figure 7a–d. Notably, under a fixed pH value, alum addition has only a weak effect on the first phase of expression, but has a substantial effect on the subsequent expression stage.

Shirato et al. (*14*) has employed the Terzaghi–Voigt combined rheological model to describe the relationship between local void ratio and local compressive pressure in the cake and has arrived at a very tedious solution for the time evolution of cake thickness. The Terzaghi–Voigt combined model is shown schematically in Figure 8 for illustration purpose. The spring in Terzaghi model accounts for the elastic behavior of consolidated cake, whose action under pressure is referred to as the "primary consolidation", while the dashpot and spring elements in the Voigt model account for the viscous behavior and is the so-called "secondary consolidation". When further assuming that the rate of primary consolidation is much higher than the secondary consolidation, which is usually the case in practice, a reduced form of solution is found as follows:

$$U_c = \frac{L_1 - L}{L_1 - L_f} = (1 - B)\left\{1 - \exp\left(-\frac{\pi^2\,\mathrm{Ce}}{4{\omega_0}^2}\theta_c\right)\right\} + B\{1 - \exp(-\eta\theta_c)\} \quad (1)$$

In eq 1, U_c is the consolidation ratio; L is the cake thickness; L_1 and L_f respectively are the initial and final cake thickness; B is the ratio of moisture removal by the secondary to total consolidation (E_2/E_1); η is the creep factor (E_2/G_2), demonstrating the easiness of the relative mobility of constituting aggregates; ω_0 is the cake volume on unit area of the filter; Ce is the consolidation coefficient, reflecting the filtration resistance of consolidated cake; θ_c is the expression time. The first and the second terms of the right-hand side of eq 1 are attributed to the primary and secondary consolidations, respectively.

The primary consolidation mechanism had been proposed to be the escape of pore liquid and the collapse of global cake structure, which corresponds to the spring rigidity (E_1) of the Terzaghi model. The secondary consolidation mechanism had been proposed to be the disturbance of the structural bonding of particles or the creeping of the particles to a more stable packing state (*26*), which correspond to the spring and dashpot elements of the Voigt model (*15*). The fraction contributed by the secondary consolidation stage is the parameter B (E_2/E_1).

As $\theta_c \rightarrow \infty$, eq 1 reduces to the following equation:

$$U_c = 1 - B\exp(-\eta\theta_c) \quad (2)$$

from which the parameters B and η can be estimated via regression analysis of the experimental data (*16–18*). A larger B value reveals a greater contribution for secondary consolidation, which is undesired for dewatering sake. A larger η value is, on the contrary, desired for the easier creeping of constituting aggregates, thereby giving less expression time to achieve the same consolidation ratio.

As indicated in Figure 7, for all sludge tests, after a decrease of U_c in the initial stage of expresssion follows a linear $\ln(1 - U_c) - \theta_c$ region. This confirmed the validity of employment of eq 2 in describing the expression characteristics for the present alum-coagulated clay slurries. The determination of the B and η values depends on the linear regression of several sets of experimental data that were conducted independently. The linear regression analysis is conducted based on *all* secondary consolidation data, which results in the best-fitting lines in Figure 7a–d with a regression coefficient exceeding 0.98. However, only one set of data is depicted in the figure to prevent confusion. Notably, the efficiency considering expression alone follows the same sequence as that for overall dewaterability: pH 5.2 > pH 3 > pH 7 > pH 10. Figures 9 and 10 represent the most opposite B and η values accompanied by the solubility curves. Both the B and η values increase with alum concentration and decrease at higher pH, while exhibiting a local minimum in charge reversal regime around pH 5–6.

Figure 11 demonstrates the microphotographs for coagulated slurries (200×). The flocs size increases markedly near neutral condition (pH 7 > pH 3 > pH 10) and at higher alum dose (only the 700 ppm dose cases are depicted for

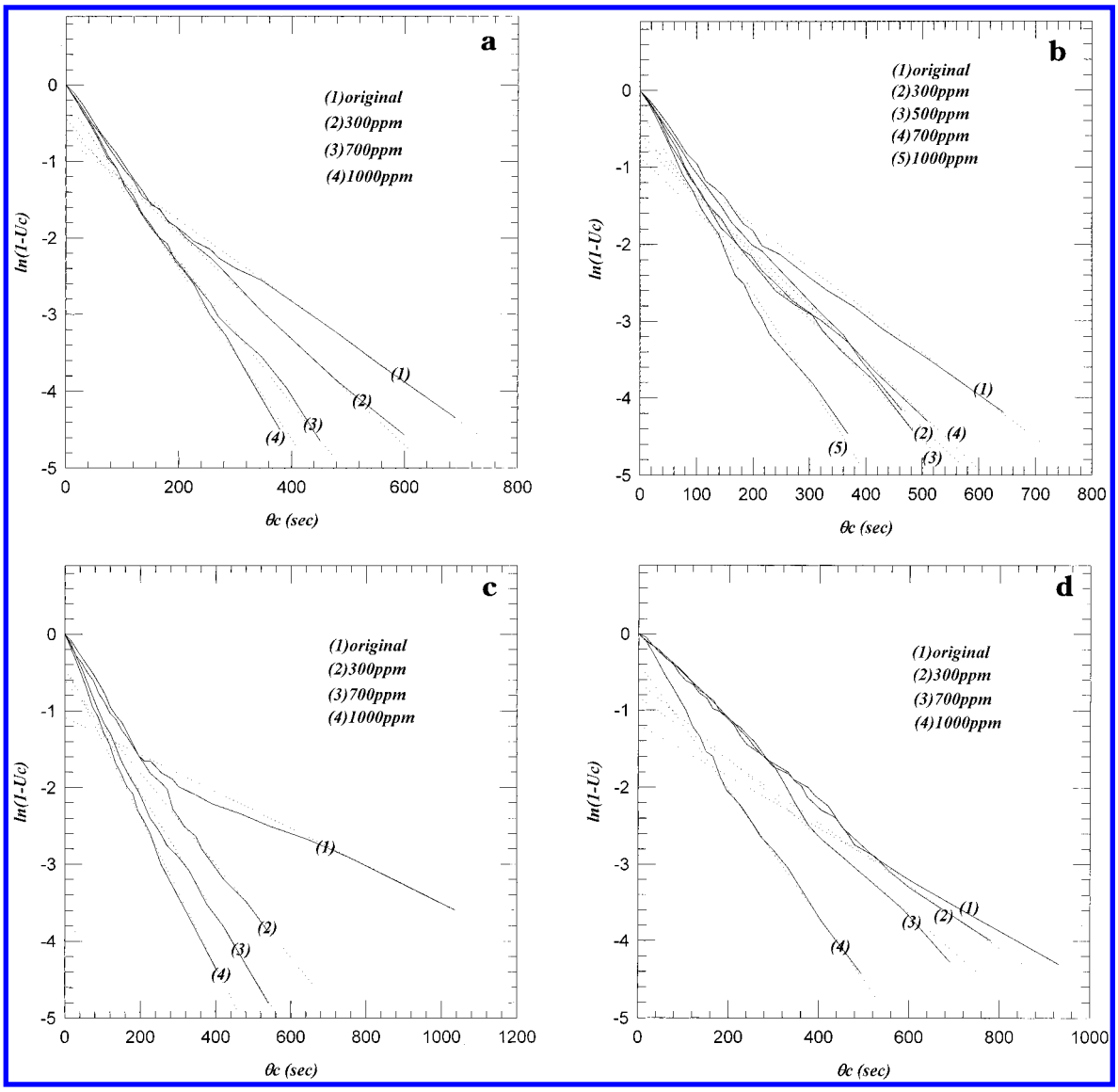

FIGURE 7. Ln (1 − U_c) versus θ_c. Clay slurry, 20% w/w, 10^{-1} N. (a) pH 3, (b) pH 5.2, (c) pH 7, and (d) pH 10.

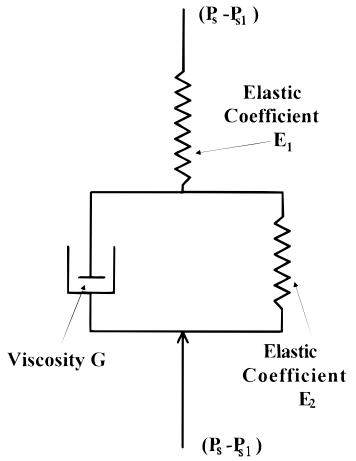

FIGURE 8. Schematics of the Terzaghi−Voigt combined rheological model.

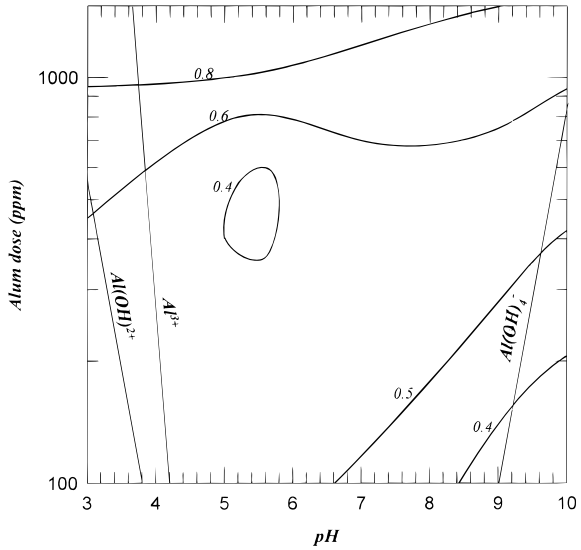

FIGURE 9. Parameter *B* on alum stability diagram.

brevity sake). The flocs with larger sizes are usually more round-shaped and compact; while those with smaller sizes are more irregular-shaped.

Alum Chemistry and Expression Characteristics. The above experimental results reveal an important role of alum chemistry on filtration and expression dewatering characteristics. The trend of B and η changes at pH 7 are similar

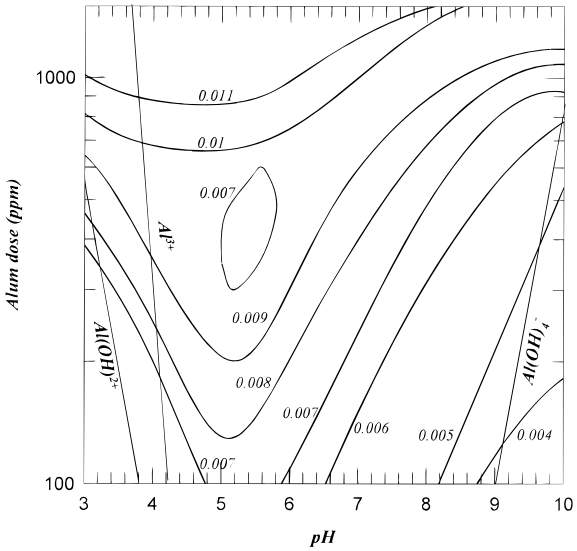

FIGURE 10. Parameter η on alum stability diagram.

to those at pH 10, i.e., the dewatering efficiency increases monotonously with alum dosage. On the other hand, the coincidence between the reversal phenomena observed for parameters B and η at pH 5.2 and the curve where ζ potential changes from negative to positive reflects the significant role of surface charge. (Note: Dewatering at pH 3 is very efficient as shown in Figure 3a, as a result, whether or not reversal in B and η occurs close to the 800 ppm dosage regime is hard to identify due to possible experimental and numerical errors.)

In the secondary consolidation stage, the ease of particles creeping is controlled by the forces acting oppositely on particles, including at least the mechanical force, the drag force exerted by the highly viscous surface water layers, and the electrostatic repulsion forces. The η is therefore an index of *inter-aggregate* interactions. By intuition, it is easy to imagine a harder passing over (creep) of a particle across the other particles with the same sign of charges due to the electrostatic repulsion. This can qualitatively explain the reversal in η observed at pH 5.2 (and maybe pH 3 as well).

However, the charge neutralization mechanism cannot explain the results at pH 7 and pH 10 since no corresponding reversal in η is observed in these tests near the charge reversal regime. The sweep floc enmeshment should correspond to the continuous increase in η as alum dose increases. As am-$Al(OH)_3$(s) appears during the sweep flocs regime, the resulting floc structure is found looser for pH 7.5 than that for pH 6.5, which is believed to be induced by different nucleation paths for crystal growth (*27*). The microphotographs shown in Figure 11 reveal that the resulting flocs at pH 7 have a nearly round shape, a compact structure, and usually large floc size (fewer aggregates on the basis of the same solid weight percent). While at pH 10, the floc exhibits irregular shape, a loose structure, and a small floc size (more aggregates exist on the basis of the same solid weight percent). Apparently, the aggregates with round shape and a compact structure can exhibit a less resistance for creeping of constituting aggregates, which corresponds to the higher η at pH 7.

A larger B value corresponds to a relatively tougher sludge cake, i.e., the sludge cake becomes more resistant to instant global structure collapse when loading is suddenly added. Independent tests had been conducted to measure the change of floc sizes of coagulated slurries applied by a 10-min ultrasonic treatment. Notably, the flocs size that can sustain ultrasonic treatment is larger at pH 7 than at pH 10, reflecting that the former exhibits a higher intra-aggregate strength. The higher B for pH 7 than pH 10 therefore corresponds to the more compact aggregate structure (*28*) and stronger intra-aggregate strength. However, reversal in B values at pH 5.2

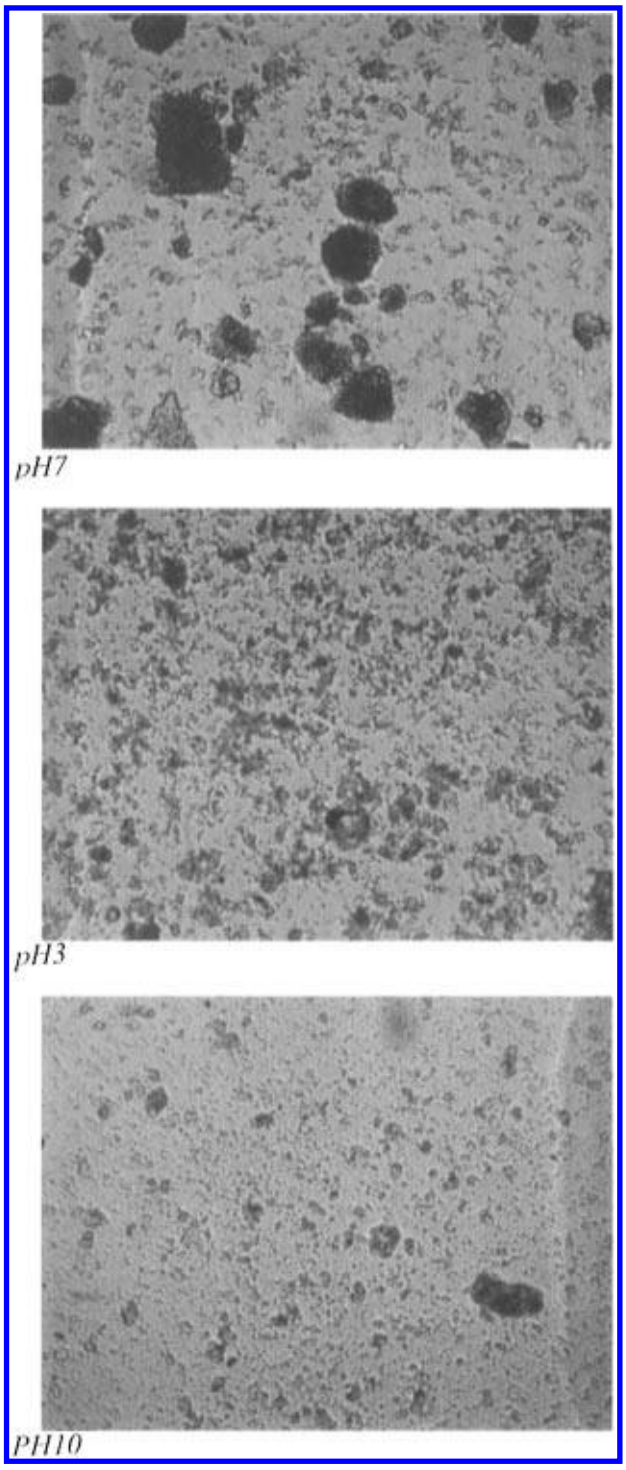

FIGURE 11. Microphotographs for alum-coagulated slurries. Alum dose 700 ppm. (a) pH 7, (b) pH 3, and (c) pH 10.

reflects the role of electrostatic repulsion in affecting global structure toughness.

The above discussions reveal that the parameters B and η are mainly controlled by intra-aggregate and inter-aggregate interactions, respectively. They might be thereby altered independently when coagulation condition changes.

Optimal Alum Dose. The optimal alum dose is usually located at the dose where the removal of turbidity (colloidal particles) or some target items (i.e., TOC) reaches a maximum (*1*, *29*−*32*). The optimal dose can be located close to the near-zero surface charge regime when the PCN mechanism is dominating (pH < 7) (point A in Figure 1). In a neutral to basic environment where sweep flocs enmeshment is domi-

nating, the optimal dose can be located at the optimal sweep zone (*10*) (point B in Figure 1). This work suggests to re-evaluate the so-called optimal alum dose considering dewatering efficiency, which apparently depends upon the specific requirement for the treatment. For example, at pH 3 (and pH 5.2 as well) where the original clay slurry dewaterability is rather good (Figure 3a,b), alum addition is deemed to be unnecessary if the reduction in filter area or the filtration time (less average specific resistance) is of major concern. On the other hand, the presence of alum can markedly enhance dewatering efficiency for pH > 7 (Figure 3c,d). An as high as possible dosage is recommended. However, if final sludge disposal of the cake after the filtration stage is the most expensive stage, a minimum filtration cake volume (the highest fraction removed in filtration stage shown in Figure 6) is desired. With such a criterion, even at pH > 7 the usually adopted optimal sweep zone is not the best choice. Actually, it needs no alum dose if considering alone the residual moisture in filtration cake. The alum addition mainly improves the turbidity removal nevertheless.

Consider the dewatering including expression stage as the succeeding dewatering procedure, such as the belt filter press practice. If the residual moisture requirement is within the range where the primary consolidation stage can reach, no specific alum dosing is preferred (the data for the first phase expression in Figure 7a−d reveal a weak dependence on alum dosage). However, if a still dryer cake is a prerequisite for final sludge disposal, the secondary consolidation dewatering stage encounters. At pH 3, no alum dose is required since the original clay slurry has exhibited a very good dewaterability. Nevertheless, in neutral to basic environment, due to the simultaneous growth of parameters B and η as alum dose increases, the optimal dose does not locate in the optimal sweep flocs regime on the basis of turbidity removal tests any more (Figures 1 and 3c,d). (Actually, an as high as possible alum dose is recommended.)

The above discussions support the arguments by Moudgil and Shah (*33*) that different aggregate characteristics are required for various intended applications. The optimal coagulant dose for sludge practice should be the specific dose that can minimize the "total" cost, including turbidity removal, settling, filtration, expression, and final disposal costs. Only if some of them (for example, the final sludge disposal) are much more expensive than the others would the corresponding optimal dose that can minimize its (sludge disposal) cost be the overall optimal one. Otherwise, an optimal dose considering the whole sludge process should be a compromise between different requirements.

Acknowledgments

This work is supported by National Science Council, Republic of China.

Literature Cited

(1) Amirtharajah, A.; Mills, K. M. *J. Am. Water Works Assoc.* **1982**, *74*, 210.
(2) James, R. O.; Wiese, G. R.; Healy, T. W. *J. Colloid Interface Sci.* **1977**, *59*, 381.
(3) Letterman, R. D.; Vanderbrook, S. G. *Water Res.* **1983**, *17*, 195.
(4) Johnson, P. N.; Amirtharajah, A. *J. Am. Water Works Assoc.* **1983**, *75*, 232.
(5) Letterman, R. D.; Iyer, D. R. *Environ. Sci. Technol.* **1985**, *19*, 673.
(6) Dentel, S. K. *Environ. Sci. Technol.* **1988**, *22*, 825.
(7) Dentel, S. K.; Gosseet, J. M. *J. Am. Water Works Assoc.* **1988**, *80*, 187.
(8) Hemme, A.; Ay, P. *Filtr. Sep.* **1994**, *31*, 647.
(9) Rebhun, M.; Lurie, M. *Water Sci. Technol.* **1993**, *27*, 1.
(10) Dentel, S. K. *Crit. Rev. Environ. Control* **1991**, *21*, 41.
(11) Tiller, F. M.; Yeh, C. S. *AIChE J.* **1987**, *33*, 1241.
(12) Vesilind, P. A. *Treatment and Disposal of Wastewater Sludges*, 2nd ed.; Ann Arbor Science: Ann Arbor, MI, 1979.
(13) Heij, E. J. La; Kerkhof, P. J. A. M.; Herwijn, A. J. M.; Coumans, W. J. *Water Res.* **1996**, *30*, 697.
(14) Shirato, M.; Murase, T.; Kato, H.; Fukaya, S. *Filtr. Sep.* **1970**, *7*, 277.
(15) Shirato, M.; Murase, T.; Tokunaga, A.; Yamada, O. *J. Chem. Eng. Jpn.* **1974**, *7*, 229.
(16) Shirato, M.; Murase, T.; Hayashi, N.; Fukushima, T. *J. Chem. Eng. Jpn.* **1977**, *10*, 154.
(17) Shirato, M.; Murase, T.; Atsumi, K.; Nagami, T.; Suzuki, H. *J. Chem. Eng. Jpn.* **1978**, *11*, 334.
(18) Shirato, M.; Murase, T.; Atsumi, K.; Aragaki, T.; Noguchi, T. *J. Chem. Eng. Jpn.* **1979**, *12*, 51.
(19) Shirato, M.; Murase, T.; Atsumi, K. *J. Chem. Eng. Jpn.* **1980**, *13*, 397.
(20) Tiller, F. M.; Yeh, C. S. *Filtr. Sep.* **1990**, *27*, 129.
(21) Yeh, S. H. Cake Deliquoring and Radial Filtration. Doctoral Dissertation, University of Houston, Houston, TX, 1985.
(22) Tong, W. C. Effects of pH Value and Chemical Conditioning on Expression of Sludges. Master Thesis, National Taiwan University, Teipei, Taiwan, 1994.
(23) Knocke, W. R.; Hamon, J. R.; Dulin, B. E. *J. Am. Water Works Assoc.* **1987**, *79*, 89.
(24) Leu, W. F. Cake Filtration. Ph.D. Dissertation. University of Houston, Houston, TX, 1981.
(25) No reference 25 given.
(26) Velamakanni, B. V.; Lange, F. F. *J. Am. Ceram. Soc.* **1991**, *74*, 166.
(27) Craig, R. F. *Soil mechanics*, 5th ed.; Chapman & Hall Publishers: London, 1992.
(28) Chowdhury, Z. K.; Amy, G. L.; Bales, R. C. *Environ. Sci. Technol.* **1991**, *25*, 1766.
(29) Vik, E. A.; Carlson, D. A.; Eikum, A. S.; Gjessing, E. T. *J. Am. Water Works Assoc.* **1985**, *77*, 58.
(30) Dolejs, P. *Water. Sci. Technol.* **1993**, *27*, 123.
(31) Vik, E. A.; Eikebrokk, B. In *Aquatic humic substances influence on fate and treatment of pollutants*; Suffet, I. H., MacCarthy, P., Eds.; ACS: Washington, DC, 1989.
(32) Dempsey, B. A.; Ganho, R. M.; O'Melia, C. R. *J. Am. Water Works Assoc.* **1984**, *76*, 141.
(33) Moudgil, B. M.; Shah, B. D. In *Advances in Solid-Liquid Separation*; Muralidhara, H. S., Eds.; Battelle Press: Columbus, OH, 1986; p 191.

Received for review June 18, 1996. Revised manuscript received December 23, 1996. Accepted January 3, 1997.[⊗]

ES9605329

[⊗] Abstract published in *Advance ACS Abstracts,* March 1, 1997.